Frontiers in Bioscience Landmark

Front. Biosci. (Landmark Ed) **2025**; 30(11): 42888
https://doi.org/10.31083/FBL42888

Original Research

Curcuma longa L. Leaf and Pseudostem Extract Suppresses Inflammation in Cytokine-Stimulated HaCaT Keratinocytes and 12-O-Tetradecanoylphorbol-13-Acetate-Induced Ear Edema in Mice

Arachchige Maheshika Kumari Jayasinghe[1], Kirinde Gedara Isuru Sandanuwan Kirindage[1], Kyungsook Jung[2], Jihye Lee[2], Seok Lee[3], Hitihami Mudiyanselage Chalani Bhagya Deshapriya[1], Hewayalage Madushika Kumari Ranasinghe[1], Lei Wang[4], Ji Soo Kim[5], Ginnae Ahn[1,6,*]

[1]Department of Food Technology and Nutrition, Chonnam National University, 59626 Yeosu, Republic of Korea
[2]Functional Biomaterials Research Center, Korea Research Institute of Bioscience and Biotechnology (KRIBB), 56212 Jeongeup-si, Republic of Korea
[3]French Korea Aromatics Co., Ltd., 16986 Yongin-si, Gyeonggi-do, Republic of Korea
[4]College of Food Science and Engineering, Ocean University of China, 266003 Qingdao, Shandong, China
[5]Division of Practical Application, Honam National Institute of Biological Resources (HNIBR), 58762 Mokpo, Republic of Korea
[6]Department of Marine Bio-Food Sciences, Chonnam National University, 59626 Yeosu, Republic of Korea
*Correspondence: gnahn@jnu.ac.kr (Ginnae Ahn)
Academic Editor: Catarina Rosado
Submitted: 4 June 2025 Revised: 18 September 2025 Accepted: 30 September 2025 Published: 20 November 2025

Abstract

Background: Plant-derived treatments for skin inflammation are gaining increasing interest, driven by the growing demand for safer alternatives to conventional synthetic drugs. *Curcuma longa* L. (turmeric) is traditionally utilized in many Asian countries for various pharmacological applications. Although the inflammation-suppressing properties of turmeric rhizomes are well established, the bioactive potential of its leaves and pseudostems remains largely unexplored. This study investigates the effects of turmeric leaf and pseudostem extract (CLE) on tumor necrosis factor (TNF)-α/interferon (IFN)-γ-stimulated HaCaT keratinocytes (HK) and 12-O-tetradecanoylphorbol-13-acetate (TPA)-induced ear edema in a mouse model. **Methods**: Cell viability and intracellular ROS levels in response to CLE were assessed. The potential of CLE to suppress inflammation was evaluated by monitoring the inhibition of signaling pathways and changes in cytokine/chemokine expression through Western blotting and real-time quantitative polymerase chain reaction (RT-qPCR) analyses. CLE was also examined for its impact on skin hydration and tight junction integrity. For *in vivo* analysis, an ear edema model was established using female BALB/c mice (7 weeks old). **Results**: CLE treatment led to a dose-dependent decline in intracellular ROS and enhanced cell viability of TNF-α/IFN-γ-stimulated HK. Treatment with CLE resulted in decreased transcription of epithelial-derived cytokines (thymic stromal lymphopoietin (TSLP), IL-25, IL-33), pro-inflammatory mediators (IL-6, IL-8, IL-13, TNF-α, IFN-γ, IL-1β), and chemokines (macrophage-derived chemokine (MDC), regulated on activation, normal T cells expressed and secreted (RANTES), thymus and activation-regulated chemokine (TARC)), along with inhibition of mitogen-activated protein kinase (MAPK) and nuclear factor kappa B (NF-κB) signaling proteins in stimulated HK. CLE improved expression of proteins associated with skin hydration and tight junctions, helping to preserve moisture balance and structural integrity. Moreover, CLE markedly reduced ear redness, swelling, and thickness in 12-O-tetradecanoylphorbol-13-acetate (TPA)-induced mice, while alleviating histopathological changes, including inflammatory cell infiltration and dermal thickening. Additionally, CLE effectively diminished inducible nitric oxide synthase (iNOS), cyclooxygenase-2 (COX-2), and pro-inflammatory cytokine expression in the ear tissues of edema-induced mice. **Conclusions**: Collectively, CLE exhibited potential as a natural anti-inflammatory agent by attenuating oxidative stress, downregulating inflammatory mediators, enhancing skin barrier function *in vitro*, and reducing ear edema *in vivo*.

Keywords: *Curcuma longa*; inflammation; keratinocytes; cytokines; edema

1. Introduction

The skin safeguards the human body by acting as the primary defense against environmental stressors. Chronic exposure to environmental stressors can impair the skin barrier, triggering inflammatory responses that disrupt skin homeostasis [1,2]. Symptoms of skin inflammation, initially acute, can progress to chronic states, contributing to the development of dermatological conditions, including rosacea, psoriasis, and atopic dermatitis [3,4]. Activation of epidermal keratinocytes and immune cells in response to external stimuli plays a central role in mediating inflammation through elevating intracellular ROS levels, promoting the release of inflammatory mediators and signaling pathways, and ultimately impairing the skin barrier. Stimulation of mitogen-activated protein kinase (MAPK) and nuclear factor kappa B (NF-κB)-mediated signaling cascades

upregulates pro-inflammatory cytokine and chemokine expression, thereby exacerbating skin inflammation and further compromising dermal hydration and intercellular tight junction integrity [5].

Accordingly, the investigation of natural compounds for treating skin inflammation has attracted increasing research attention. Previous studies have shown that anti-inflammatory plant extracts may serve as promising treatments for cutaneous inflammation by regulating inflammatory mediator expression and reducing cellular damage [6,7]. *Curcuma longa* L. (turmeric), a rhizomatous perennial herb, is widely distributed across tropical and subtropical regions, with particular prevalence in Asia [8]. Turmeric has been used as a medicinal herb since ancient times to mitigate and manage a wide range of conditions, including common colds, wounds, skin sores, diarrhea, throat infections, urinary tract infections, menstrual problems, digestive disorders, and liver diseases [9]. It has been extensively used for centuries in Ayurveda (India), Unani (Pakistan), and traditional medicine in Bangladesh for its diverse therapeutic properties, with records of use in India dating back at least 2500 years [10]. Accordingly, research has confirmed the pharmacological relevance of turmeric by identifying numerous bioactive phytochemicals, including curcumin, terpenes, phytosterols, flavonoids, and other phenolic compounds, in various plant parts, which exhibit anti-allergic, anti-atopic dermatitis, antioxidant, antibacterial, and anti-tumor activities [8,11]. Although considerable progress has been achieved, most investigations have concentrated on the turmeric rhizome. Data on the chemical composition, bioactivities, and therapeutic relevance of the aerial parts, particularly leaves and pseudostems remain limited. Their potential roles in modulating skin inflammation, redox homeostasis, and immune regulation have not been fully elucidated, emphasizing a critical knowledge gap that the present study seeks to address.

In line with this, our collaborative study identified twenty-one phenolic compounds in turmeric leaf and pseudostem extract (CLE) [12]. Furthermore, we previously examined the pharmacological effects of CLE against allergic responses and atopic dermatitis using both cell-based and organismal models [8,13]. Building on previous studies, this work focuses on exploring the effects of CLE on inflammatory responses in the skin using both cellular and animal models. Thus, the current study investigates the inflammation-regulating properties of CLE *in vitro*, using tumor necrosis factor (TNF)-α/interferon (IFN)-γ-treated HaCaT keratinocytes (HK), and *in vivo*, through a 12-O-tetradecanoylphorbol-13-acetate (TPA)-induced ear edema mouse model.

2. Materials and Methods

2.1 Chemicals/Reagents

Dulbecco's Modified Eagle Medium (DMEM), fetal bovine serum (FBS), and a penicillin/streptomycin mixture were obtained from GibcoBRL (Grand Island, NY, USA). Sigma-Aldrich (St. Louis, MO, USA) supplied 3-(4,5-dimethylthiazol-2-yl)-2,5-diphenyltetrazolium bromide (MTT), 2′,7′-dichlorodihydrofluorescein diacetate (DCF-DA), dimethyl sulfoxide (DMSO), paraformaldehyde, Triton™ X-100, TRIzol, indomethacin (IM), and TPA. Thermo Fisher Scientific (Rockford, IL, USA) provided the protein ladder, NE-PER® nuclear/cytoplasmic extraction kit, and Pierce™ RIPA buffer. Primers were acquired from Bioneer Co. (Daedeok-gu, Daejeon, Korea). Recombinant TNF-α and IFN-γ were purchased from R&D Systems (Minneapolis, MN, USA). Reagents and chemicals not specified above were of analytical grade. The identification of *C. longa* L. and the CLE extraction procedure were described in a previous study [13]. According to the findings from a collaborating research group, liquid chromatography-electrospray ionization-mass spectrometry (LC-ESI-MS) analysis identified twenty-one phenolic compounds in CLE [12].

2.2 Cells

HK were originally purchased from the Korean Cell Line Bank (KCLB, Seoul, Korea). Short Tandem Repeat (STR)-verified, mycoplasma-free cells were maintained at 37 °C in 5% CO_2 under humidified conditions, using DMEM supplemented with 10% heat-inactivated FBS and 1% penicillin/streptomycin. Subcultures were performed when the cells reached 70–80% confluence, and experiments were conducted during the exponential growth phase.

2.3 Assessment of Cell Viability and Intracellular ROS Levels

Cell viability in response to CLE treatment was evaluated using the MTT assay. After treatment with CLE for 2 h, cells were stimulated for 24 h with a 1:1 mixture of TNF-α and IFN-γ (final concentration of 10 ng/mL). Following 4 h of treatment with MTT reagent, DMSO was added to the cells. The absorbance at 570 nm was determined using a SpectraMax M2 microplate reader (Molecular Devices, Silicon Valley, CA, USA) after 30 min of incubation.

Intracellular ROS levels in response to CLE treatment were assessed through the DCF-DA assay. For this experiment, cells were first incubated with CLE for 2 h, followed by DCF-DA treatment. Fluorescence emission was detected using SpectraMax M2 equipment and further analyzed with a CytoFLEX flow cytometer (Beckman Coulter, Brea, CA, USA).

2.4 RT-qPCR and ELISA Analyses

As described in Kirindage *et al.* [14], cDNA was synthesized from total RNA using a ReverTra cDNA synthesis kit (FSQ-101, Toyobo, Osaka, Japan). Gene amplification by real-time quantitative polymerase chain reaction (RT-qPCR) was performed using PowerSYBR® Green PCR Master Mix (Applied Biosystems, Life Technologies,

Warrington, UK), according to the manufacturer's guidelines. The relative changes in gene expression were determined using the $2^{-\Delta\Delta CT}$ approach and comparing each gene's expression level to that of GAPDH. **Supplementary Table 1** provides the primer sequences used for RT-qPCR. Hyaluronic acid (HA) levels were quantified with an ELISA kit (DHYAL0, R&D Systems, Inc., Minneapolis, MN, USA).

2.5 Western Blot (WB) Analysis

Protein samples (30 µg each) were resolved on a 10% polyacrylamide gel and subsequently transferred onto nitrocellulose membranes, as described previously [15]. Blocking of membranes was performed using 5% skimmed milk, and incubation with primary monoclonal antibodies (1:1000) was carried out at 4 °C for 12 h. After washing, membranes were transferred into secondary antibody solutions (1:3000) and incubated for 2 h. Protein bands were imaged with a Davinch Mini Chemi Imaging system (Model: MW 420, Core Bio Davinch, Seoul, Korea). WB primary antibodies, p-p38: #9211, p38: #8690, p-ERK: #4377, ERK: #9102, p-JNK: #9251, JNK: #9252, IκBα: #4812, p-IκBα: #2859, NF-κB p65: #8242, p-NF-κB p65: #3033, claudin 1: #4933, NOS: #2977, and COX-2: #4842 were purchased from Cell Signaling Technology (Danvers, MA, USA). Lympho-epithelial Kazal-type-related inhibitor (LEKTI): sc-137109, protease-activated receptor 2 (PAR-2): sc-13504, and involucrin: sc-21748 were obtained from Santa Cruz Biotechnology, Inc. (Dallas, TX, USA). Kallikrein-5 (KLK5): ab168340, phospholipase A2 (PLA-2): ab139692, claudin 4: ab53156, claudin 7: ab27487, claudin 23: ab23355, occludin: ab168986, and zonula occludens-1 (ZO-1): ab216880 were supplied by Abcam plc, Cambridge, UK. Lamin B: PA5-19468 antibody was provided by Thermo Fisher Scientific (Rockford, IL, USA). β-actin: A5316 was purchased from Sigma-Aldrich (St. Louis, MO, USA). Filaggrin: #905801 antibody was obtained from BioLegend (San Diego, CA, USA). WB secondary antibodies, goat anti-mouse IgG (G21040), and goat anti-rabbit IgG (G21234) were obtained from Thermo Fisher Scientific (Rockford, IL, USA).

2.6 Immunofluorescence Analysis

Cells grown on chamber slides were rinsed with PBS before fixation in 4% formaldehyde. Following treatment with a blocking buffer, they were exposed to the primary anti-NF-κB p65 antibody (#8242, Cell Signaling Technology, Danvers, MA, USA), and then to the corresponding goat anti-rabbit IgG secondary antibody (G21234, Thermo Fisher Scientific, Rockford, IL, USA). Coverslips were mounted with ProLong Gold antifade reagent containing DAPI, and fluorescence images were acquired on an EVOS M5000 imaging system (Thermo Fisher Scientific, Rockford, IL, USA).

2.7 TPA-induced Ear Edema

Seven-week-old female BALB/c mice, supplied by Orient Bio, Inc. (Gwangju, Korea), were used in this study. Environmental conditions were regulated (23 $\pm$ 2 °C, 55 $\pm$ 10% humidity, 12 h light/dark cycle), and animals were given food and water freely and randomly divided into five groups; the normal group (control, n = 6), TPA group (only TPA [2.5 µg/ear] applied mice, n = 6), CLE 50 µg/ear group (TPA + CLE 50 µg/ear applied mice, n = 6), CLE 100 µg/ear group (TPA + CLE 100 µg/ear applied mice, n = 6), and positive control (PC)/IM group (TPA + IM 50 µg/ear applied mice, n = 6). Both the inner (10 µL) and outer (10 µL) surfaces of each mouse ear were topically treated with CLE and IM (diluted in 100% acetone). TPA (2.5 µg/20 µL of 100% acetone/ear) was topically applied to each mouse's inner (10 µL) and outer (10 µL) ear surfaces after 1 h of CLE treatment to induce edema. After 48 h, the redness and swelling of the ears were assessed. A digital caliper with a resolution of 0.01 mm was used to determine ear thickness. Following the ear thickness measurement, mice were euthanized by isoflurane overdose using the open-drop technique, in which anesthetic-soaked gauze was placed in a sealed chamber without direct contact with the mice, in accordance with AVMA guidelines. Briefly, mice were placed in a transparent chamber equipped with an oxygen meter, pre-flushed with oxygen, and isoflurane was administered at $\geq$5% (v/v) for overdose (carrier gas: 100% O_2). Death was confirmed by cervical dislocation.

2.8 Histological Analysis

The histology of mouse ear tissues treated with TPA was examined following a method described in an earlier study [16]. In brief, ear tissues were fixed in formalin, dehydrated, embedded in paraffin, and sectioned at a thickness of 5 µm. Sections were deparaffinized (12 h, 40 °C), rehydrated, and stained with H&E solution (Abcam plc, Cambridge, UK). Mounted slides were visualized using a bright-field microscope (DM5000 B, Leica, Wetzlar, Germany).

2.9 Statistical Analysis

Statistical evaluations were conducted using GraphPad Prism software, version 10.4.2 (Boston, MA, USA). Data are presented as the mean $\pm$ standard deviation (SD), and differences with $p < 0.05$ were regarded as statistically significant. Comparisons among groups were analyzed by one-way ANOVA followed by Tukey's post hoc test.

3. Results

3.1 CLE Increased Cell Viability and Suppressed Intracellular ROS Levels

CLE showed no significant cytotoxicity at the tested concentrations in HK, as shown in Fig. 1A. Conversely, CLE significantly enhanced viability of stimulated HK, within the concentration range of 31.3 µg/mL–125 µg/mL

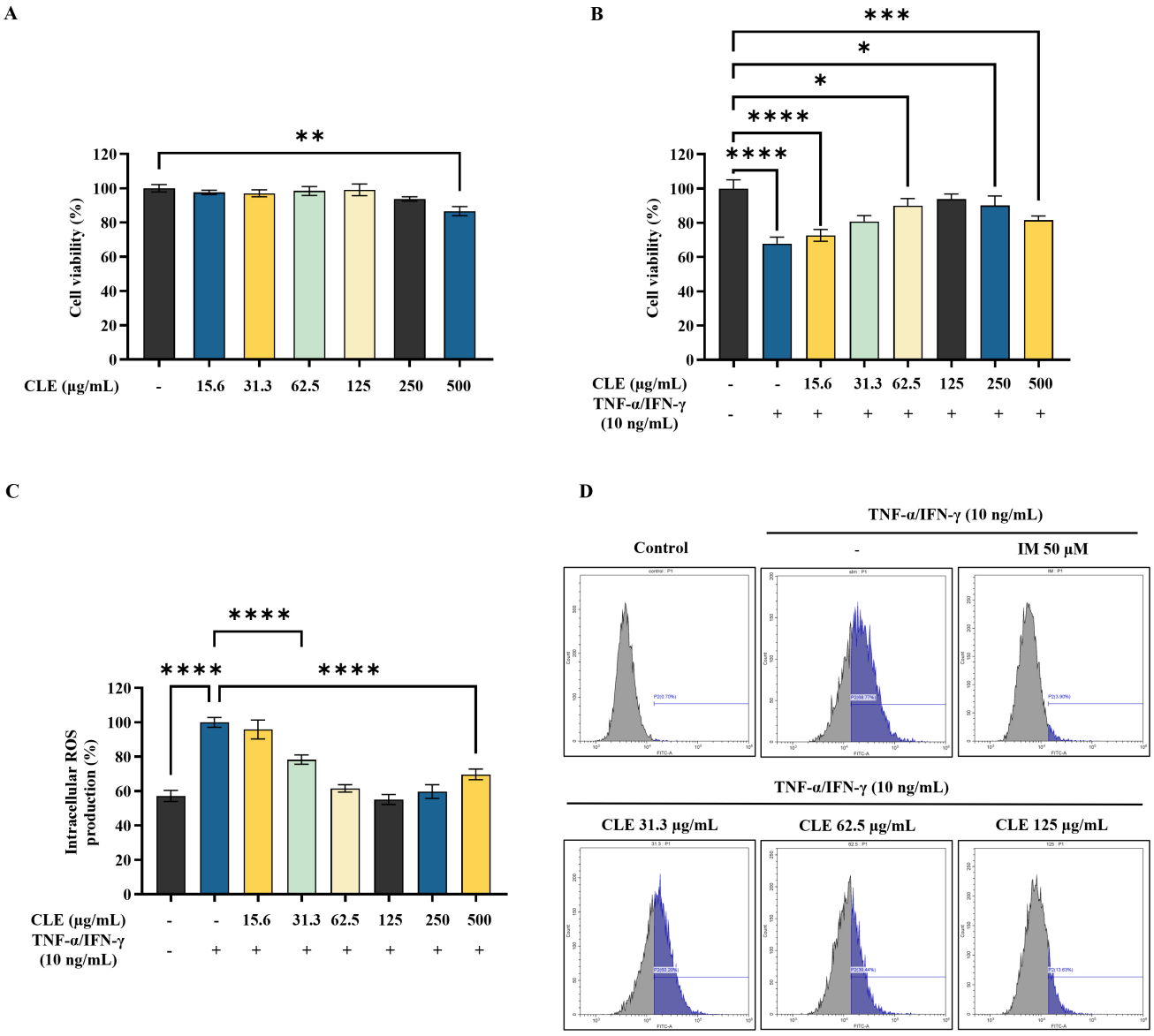

Fig. 1. Protective effect of CLE in TNF-α/IFN-γ-stimulated HK. (A) Evaluation of CLE cytotoxicity was carried out at doses between 15.6 and 500 µg/mL. (B) Evaluation of CLE's effects on cell viability in HK stimulated with TNF-α/IFN-γ (final concentration of 10 ng/mL) for 24 h, using the MTT assay. Analysis of ROS production in TNF-α/IFN-γ-stimulated HK for 1 h, assessed by DCF-DA using (C) fluorometric and (D) flow cytometric assays. Values are presented as mean ± SD, based on three separate experiments (n = 3). *$p <$ 0.05, **$p < 0.01$, ***$p < 0.001$, ****$p < 0.0001$. CLE, turmeric leaf and pseudostem extract; HK, HaCaT keratinocytes; MTT, 3-(4,5-dimethylthiazol-2-yl)-2,5-diphenyltetrazolium bromide; DCF-DA, 2′,7′-dichlorodihydrofluorescein diacetate; TNF-α, tumor necrosis factor-α; IFN-γ, interferon-γ; ROS, reactive oxygen species.

(Fig. 1B). As presented in Fig. 1C, DCF-DA staining revealed that CLE progressively lowered intracellular ROS levels with increasing doses, which was further validated by flow cytometric analysis (Fig. 1D).

3.2 CLE Downregulated the mRNA Expression of Inflammatory Mediators

Stimulation with TNF-α/IFN-γ led to an upregulation of epithelial-derived cytokines, such as thymic stromal lymphopoietin (TSLP), IL-25, and IL-33, as verified by RT-qPCR (Fig. 2A). However, CLE treatment resulted in diminished expression of these cytokines. Moreover, CLE suppressed pro-inflammatory cytokine gene expression (IL-6, IL-8, IL-13, TNF-α, IFN-γ, and IL-1β) in stimulated HK (Fig. 2B). As shown in Fig. 2C, CLE treatment led to a dose-related reduction in the chemokines macrophage-derived chemokine (MDC), regulated on activation, normal T cells expressed and secreted (RANTES), and thymus and activation-regulated chemokine (TARC). To examine the time-dependent anti-inflammatory activity

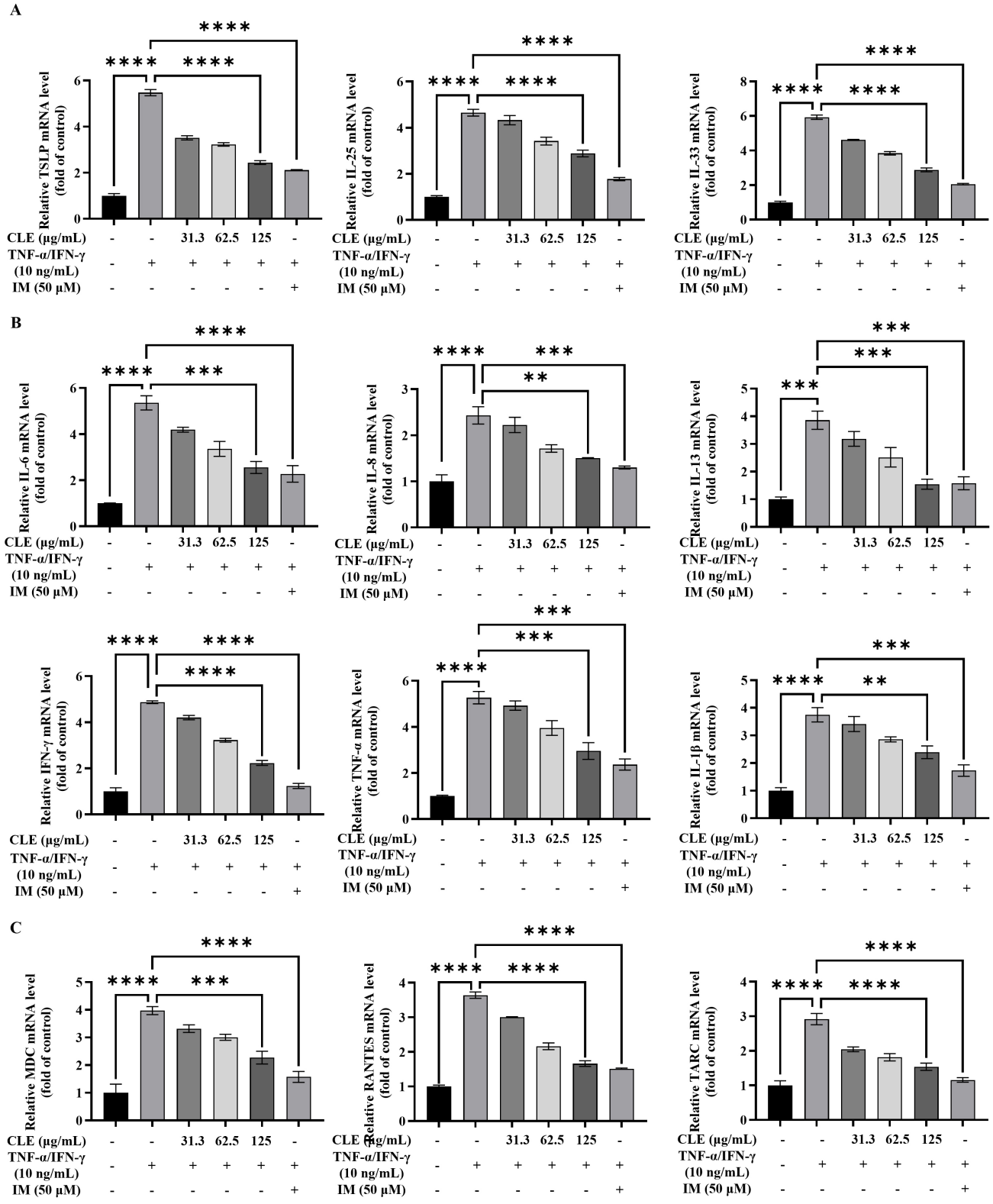

Fig. 2. CLE suppressed the expression of inflammatory mediators in TNF-α/IFN-γ-stimulated HK. RT-qPCR was performed to evaluate the mRNA levels of (A) epithelial-derived cytokines, (B) pro-inflammatory cytokines, and (C) chemokines. HK were stimulated with TNF-α/IFN-γ (final concentration of 10 ng/mL) for 12 h–24 h before harvest. Relative mRNA expression levels were normalized to the control (unstimulated cells) and are presented as fold changes. Values are presented as mean ± SD, based on three separate experiments (n = 3). $^{**}p < 0.01$, $^{***}p < 0.001$, $^{****}p < 0.0001$. IM, indomethacin; RT-qPCR, real-time quantitative polymerase chain reaction.

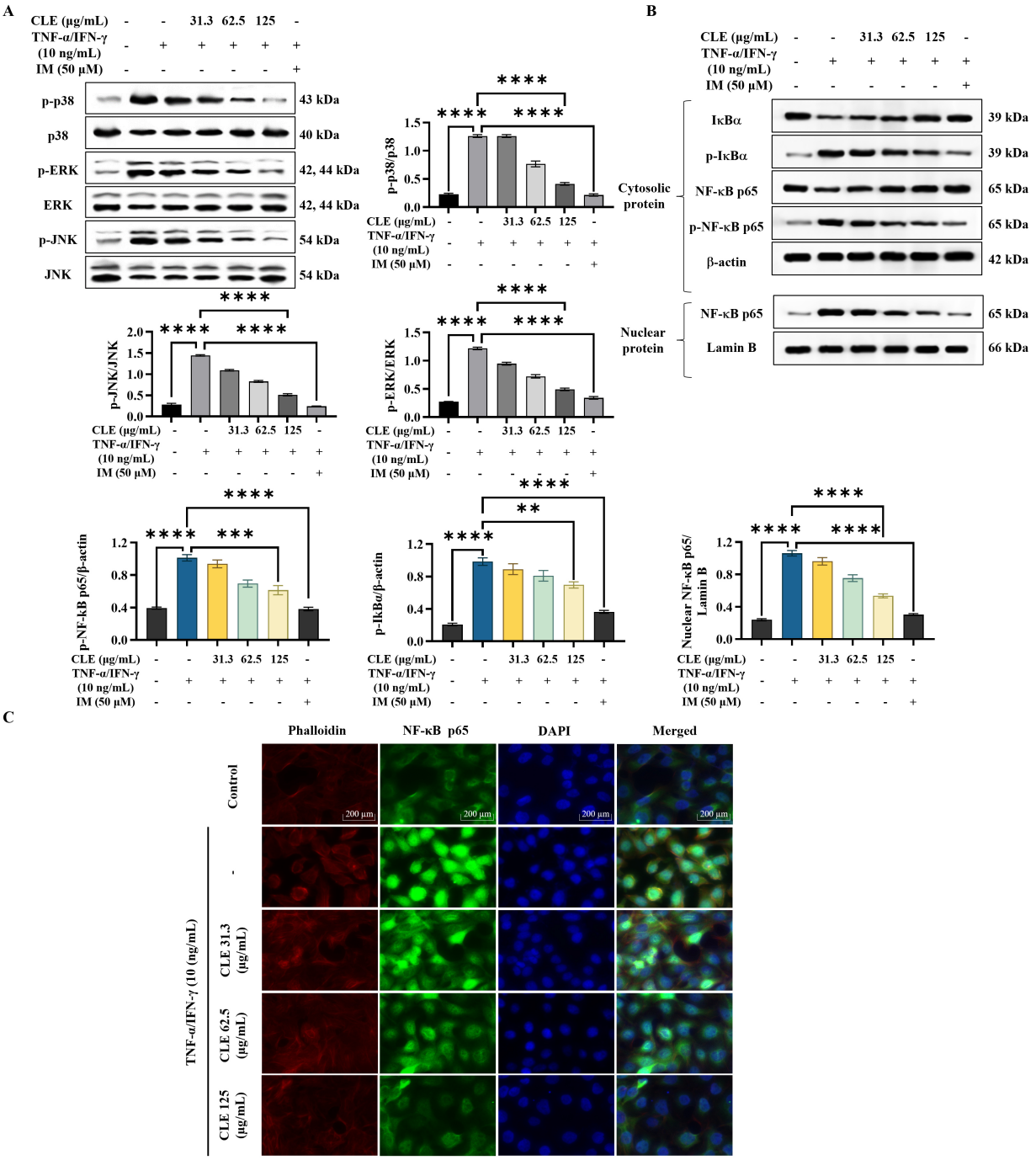

Fig. 3. CLE attenuated the activation of inflammatory pathways in TNF-α/IFN-γ-stimulated HK. WB analysis of (A) MAPK, (B) NF-κB signaling. (C) Immunofluorescence detection of NF-κB p65 translocation to the nucleus (scale bar: 200 μm). HaCaT keratinocytes were stimulated with TNF-α/IFN-γ (final concentration of 10 ng/mL) for 30 mins for immunofluorescence analysis, and until harvest for WB. For immunofluorescence, all groups were imaged under the same instrumental settings to allow direct comparison of p65 nuclear translocation. Values are presented as mean ± SD, based on three separate experiments (n = 3). $^{**}p < 0.01$, $^{***}p < 0.001$, $^{****}p < 0.0001$. WB, Western blot.

of CLE, HK were exposed to TNF-α/IFN-γ and harvested after 6, 12, and 24 h of stimulation. At all examined time points, stimulation with TNF-α/IFN-γ markedly elevated IL-6, TNF-α, and IL-1β expression levels. Treatment with CLE resulted in a significant decline in mRNA levels of these inflammatory markers, most prominently at 12 and 24 h (**Supplementary Fig. 1**). These findings indicate that CLE progressively attenuates cytokine mRNA expression over time.

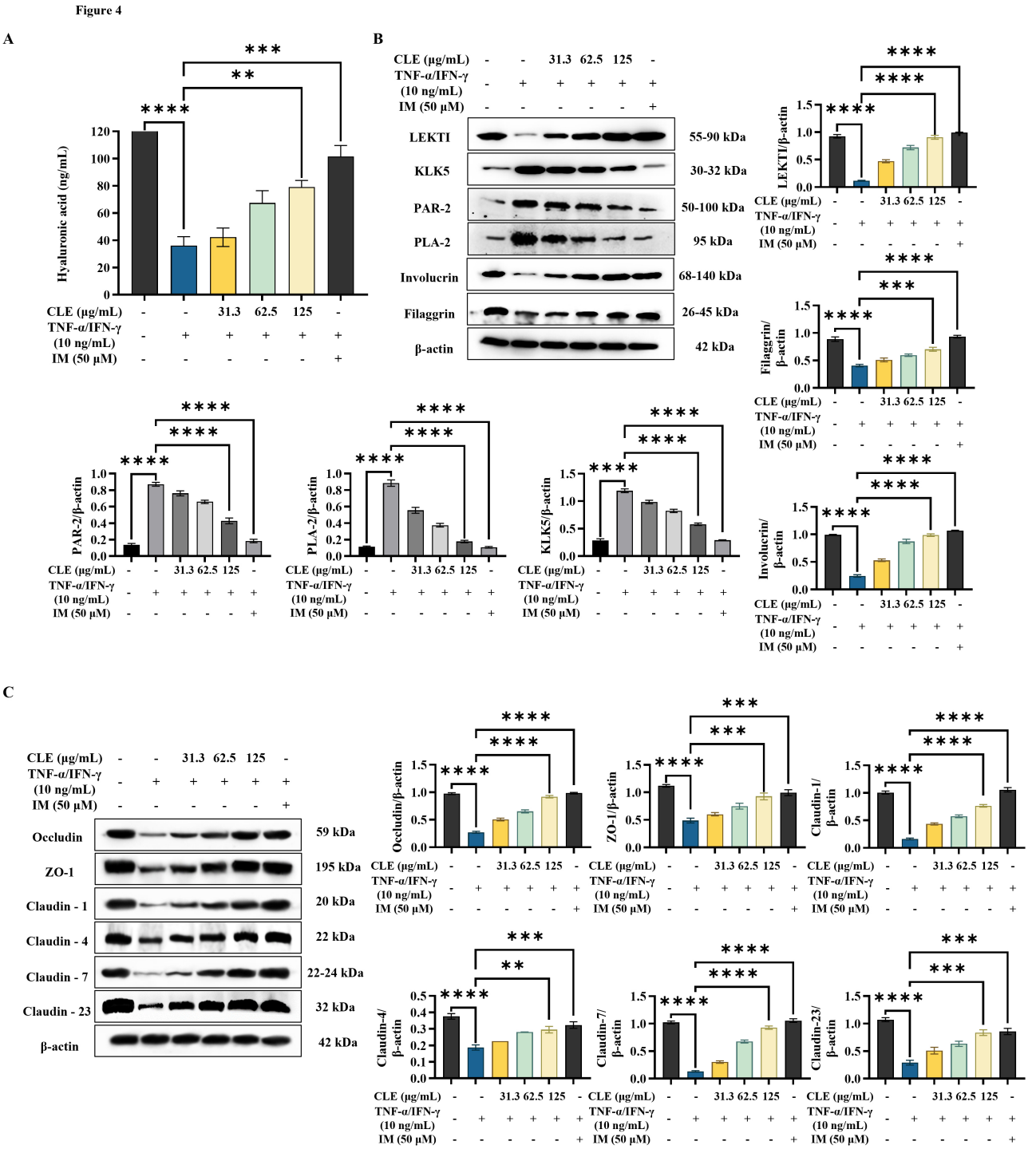

Fig. 4. CLE improved the integrity of the epidermal barrier in TNF-α/IFN-γ-stimulated HK. (A) ELISA of HA production. WB analysis of (B) protein associated with skin hydration and (C) tight junction components. HK were stimulated with TNF-α/IFN-γ (final concentration of 10 ng/mL) for 24 h before harvest for WB. HA production was measured using ELISA after 24 h of stimulation. Values are presented as mean ± SD, based on three separate experiments (n = 3). $^{**}p < 0.01$, $^{***}p < 0.001$, $^{****}p < 0.0001$. HA, hyaluronic acid.

3.3 CLE Regulated MAPK/NF-κB Signaling Pathways

As shown in the WB results (Fig. 3A), stimulation with TNF-α/IFN-γ enhanced the phosphorylation levels of p38, ERK, and JNK MAPK proteins, whereas CLE dose-dependently reduced their phosphorylation. Additionally, following TNF-α and IFN-γ stimulation, cytosolic IκBα and NF-κB p65 phosphorylation was increased, with NF-κB p65 translocating to the nucleus. However, CLE

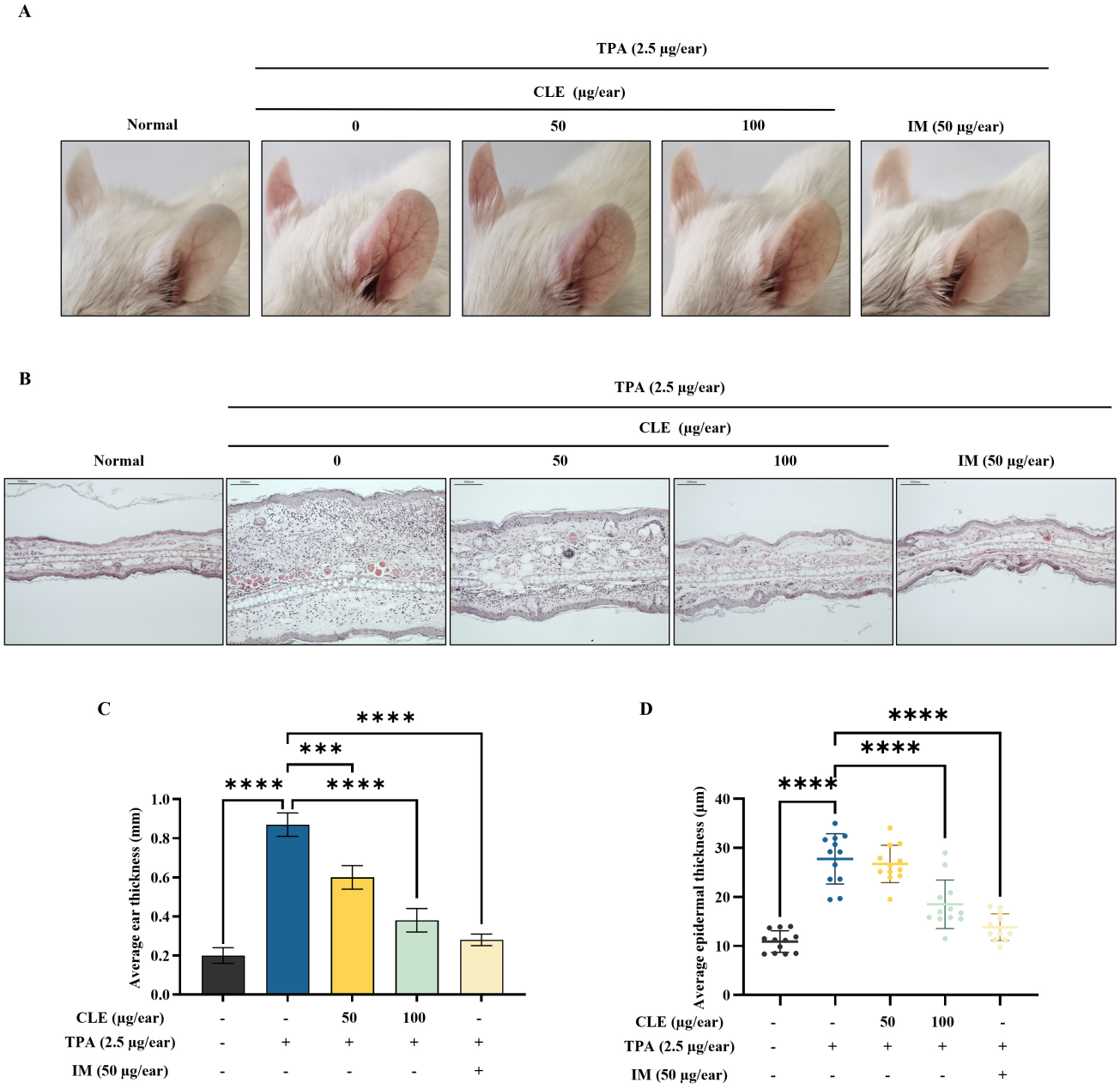

Fig. 5. CLE reduced TPA-induced ear edema in BALB/c mice. (A) Representative images of the ears and swelling in edema mice. (B) Histological evaluation of ear tissues was performed with H&E staining (scale bar: 100 μm). Alterations in (C) mouse ear thickness and (D) epidermal thickness. Values are presented as mean ± standard deviation (n = 6 mice per group). ***$p < 0.001$, ****$p < 0.0001$.

markedly suppressed these phosphorylation events and inhibited NF-κB p65 nuclear translocation (Fig. 3B). Furthermore, reduced green fluorescence intensity indicated that CLE inhibited nuclear localization of NF-κB p65, confirmed by immunofluorescence staining (Fig. 3C).

3.4 CLE Upregulated the Skin Barrier Function

According to ELISA analysis results (Fig. 4A), TNF-α/IFN-γ reduced HA production, whereas CLE significantly increased it. While CLE decreased the expression of KLK5, PAR-2, and PLA-2 in stimulated HK, it dose-dependently increased the skin moisture-related protein expression, such as LEKTI, involucrin, and filaggrin (Fig. 4B). Moreover, CLE increased the levels of several tight junction proteins, such as occludin, ZO-1, and multiple claudins (claudin-1, -4, -7, and -23), in a dose-dependent manner (Fig. 4C).

3.5 CLE Attenuated the TPA-induced Ear Edema in Mice

Fig. 5A shows representative images of ear redness and swelling in mice with edema. Accordingly, CLE visibly reduced ear redness and swelling in TPA-

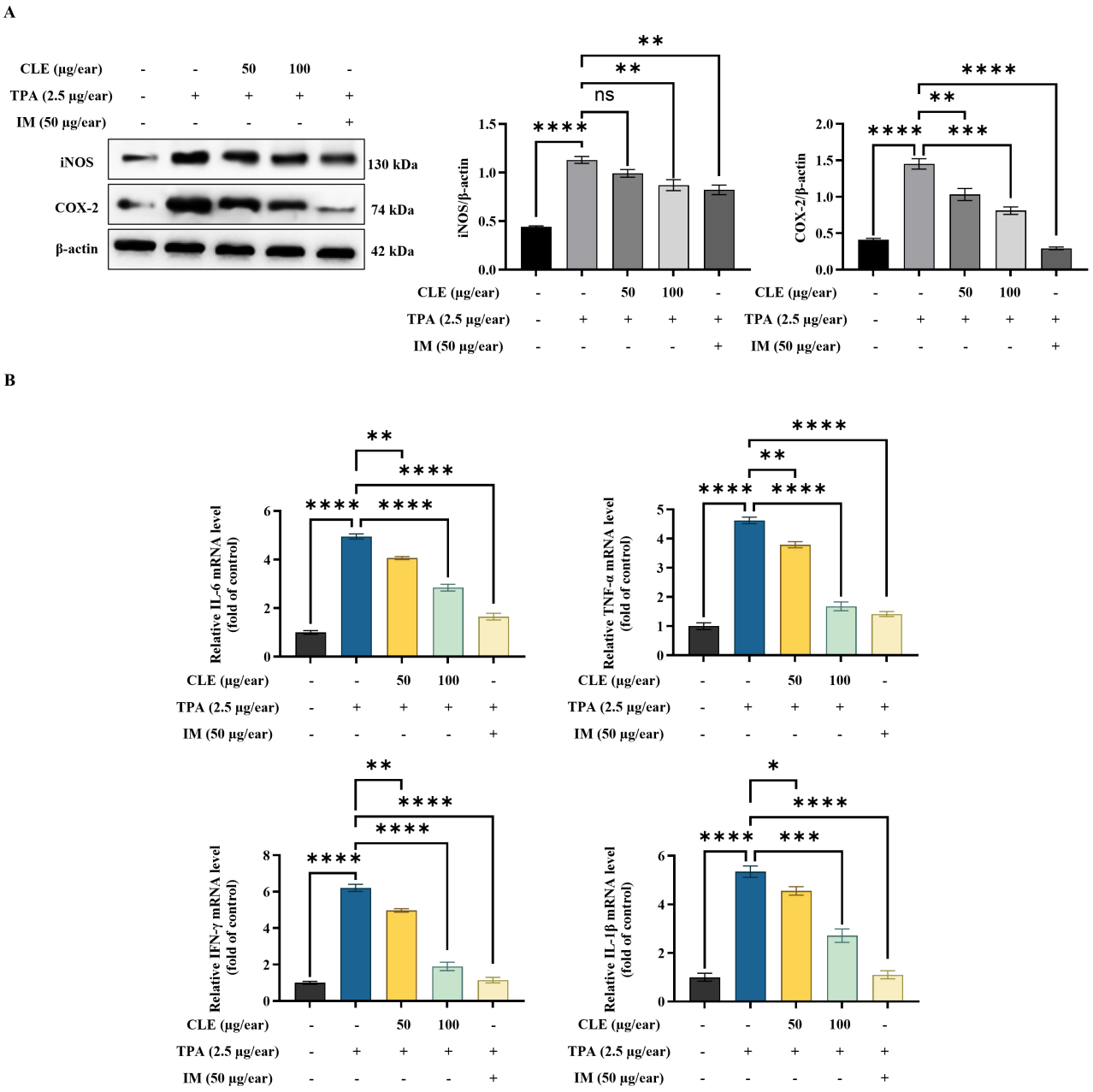

Fig. 6. CLE decreased inflammatory mediators in ear edema tissues. (A) WB of iNOS/COX-2 protein expression. (B) Analysis of pro-inflammatory cytokine mRNA expression levels using RT-qPCR. Relative mRNA levels were expressed relative to the control group and are presented as fold changes. Values are presented as mean ± standard deviation (n = 6 mice per group). *$p < 0.05$, **$p < 0.01$, ***$p < 0.001$, ****$p < 0.0001$, ns - not significant. iNOS, inducible nitric oxide synthase; COX-2, cyclooxygenase-2.

induced mice. H&E-stained ear tissue sections provided additional evidence supporting CLE's anti-inflammatory activity. The TPA application increased inflammatory cell infiltration compared with the control. CLE dose-dependently alleviated these histopathological changes (Fig. 5B). Ear thickness measurements showed that TPA application significantly increased ear swelling, indicating severe edema. However, CLE reduced ear thickness in mice in a concentration-dependent fashion (Fig. 5C). H&E-stained ear sections were analyzed to quantify epidermal thickness using image processing software (ImageJ, National Institute of Health, MD, USA), showing that CLE treatment reduced epidermal thickening in edema mice (Fig. 5D).

3.6 CLE Downregulated iNOS/COX-2, and Inflammatory Cytokines Expression in TPA-induced Mouse Ear Tissues

According to WB analysis, TPA increased inducible nitric oxide synthase (iNOS) and cyclooxygenase-2 (COX-2) protein expression in ear tissues (Fig. 6A). However,

CLE effectively reduced the expression of these proteins in ear edema tissues. Furthermore, TPA application significantly enhanced the transcription of pro-inflammatory cytokines (IL-6, TNF-α, IFN-γ, and IL-1β) in ear tissues. In contrast, CLE diminished it in a dose-dependent fashion (Fig. 6B).

4. Discussion

The identification of plant-derived anti-inflammatory treatments for skin inflammation is essential, given the growing demand for safer and more sustainable alternatives to synthetic drugs. Conventional treatments, such as corticosteroids, are effective but can cause adverse effects with prolonged or inappropriate use. These effects include skin atrophy, telangiectasias, and other local or systemic complications, highlighting the need for bioactive compounds with minimal toxicity [17]. Natural extracts, particularly those rich in polyphenols and flavonoids, have demonstrated both antioxidant capacity and anti-inflammatory properties [18,19]. According to a collaborating research group, four major compounds, vanillic acid, *p*-coumaric acid, 4-methylcatechol, and afzelin, were quantified among the 21 phenolic compounds identified in CLE by LC-ESI-MS analysis. Their quantified contents were 0.431 $\pm$ 0.002 mg/g for *p*-coumaric acid, 0.199 $\pm$ 0.001 mg/g for 4-methylcatechol, 0.129 $\pm$ 0.000 mg/g for vanillic acid, and 0.074 $\pm$ 0.000 mg/g for afzelin [12]. Earlier research has extensively reported the anti-inflammatory effects of these phenolic compounds [20–23]. For instance, a study demonstrated that vanillic acid possesses anti-inflammatory activity in lipopolysaccharide-stimulated mouse peritoneal macrophages through the inhibition of NF-κB signaling, stabilization of IκBα, and reduction of caspase-1 activity [24]. *p*-Coumaric acid has been reported to exhibit notable anti-inflammatory activity in adjuvant-induced arthritic rats by decreasing TNF-α levels and circulating immune complexes, supporting its potential role in the overall activity of CLE [25]. Furthermore, 4-methylcatechol has demonstrated anti-inflammatory activity in a rheumatoid arthritis model by suppressing pro-inflammatory cytokines, inhibiting M1 macrophage polarization, and modulating the NF-κB pathway [22]. Afzelin effectively reduces the proinflammatory effects induced by particulate matter in human keratinocytes [23]. Findings of our study demonstrate the inflammation-modulating effects of CLE may arise from the synergistic or additive actions of these bioactive compounds. This potential highlights their promise as candidates for skin-protective therapies.

Aging and skin inflammation are strongly influenced by the accumulation of cellular ROS. Our analysis revealed that stimulated HK displayed markedly elevated ROS accumulation. Nevertheless, CLE dose-dependently suppressed intracellular ROS accumulation. A comparable reduction in ROS levels has also been reported with pure compounds in cytokine-stimulated HK [15]. This finding suggests a promising avenue for further investigation into their potential anti-inflammatory properties. TSLP, IL-25, and IL-33 are key cytokines that regulate immune responses in inflamed skin. These molecules activate both innate and adaptive immunity, playing a crucial role in promoting inflammation and tissue remodeling [15]. The outcomes of the study demonstrated that CLE markedly downregulated the mRNA expression levels of above cytokines in *in vitro* RT-qPCR. These findings align with earlier reports describing the skin's anti-inflammatory mechanisms [26]. Furthermore, IL-6 and IL-8 facilitate the immune cells recruitment to sites of inflammation [27,28]. TNF-α and IFN-γ strengthen inflammatory cascades, while IL-1β exacerbates tissue damage by activating pro-inflammatory signaling. Moreover, RANTES and TARC contribute to chronic inflammation by promoting T-cell recruitment [29]. CLE noticeably reduced the mRNA expression of chemokines, epithelial cytokines, and pro-inflammatory mediators. The observations correspond with previous reports demonstrating the anti-inflammatory effects of plant-derived extracts [30].

The NF-κB/MAPK pathways drive inflammatory mediator expression, and their inhibition offers a promising strategy to mitigate skin inflammation and tissue damage [5,16]. The investigation revealed that CLE treatment markedly inhibited NF-κB p65 phosphorylation and its nuclear translocation stimulated HK. Additionally, suppression of MAPK phosphorylation confirmed that CLE inhibits NF-κB/MAPK signaling involved in inflammation. A previous review highlighted turmeric and its active compounds as modulators of these pathways in inflammatory disorders and pain, thereby supporting the relevance of the present findings [31].

Similarly, preserving skin barrier integrity is crucial for controlling inflammation, as it depends on HA production, the regulation of skin moisturization-related proteins, and the activity of tight junction proteins, factors that collectively support hydration, barrier stability, and immune defense [32]. HA promotes hydration and tissue repair, while moisturization-regulating proteins sustain epidermal homeostasis. Tight junction proteins further strengthen barrier function, limiting antigen penetration and immune hyperactivation [5,33]. Nevertheless, pro-inflammatory cytokines, primarily controlled through NF-κB and MAPK signaling pathways, disrupt these protective mechanisms and exacerbate skin damage [34]. In this study, TNF-α/IFN-γ stimulation of HK resulted in decreased expression of involucrin, filaggrin, and LEKTI, key proteins involved in epidermal barrier formation, cell adhesion, and skin desquamation regulation. However, CLE pretreatment enhanced LEKTI, involucrin, and filaggrin expression, while suppressing KLK5, PAR-2, and PLA-2, thereby supporting its role in promoting skin hydration. These findings suggest that CLE protects against TNF-α/IFN-γ-induced moisture loss, consistent with outcomes reported

in a previous study [5]. Furthermore, administration of CLE replenished HA levels and upregulated tight junction proteins such as occludin, ZO-1, and multiple claudins (claudin-1, -4, -7, and -23), thereby reinforcing its role in preserving skin barrier function during inflammation.

In *in vivo* studies, epithelial- and epidermal-derived innate cytokines are upregulated during innate immune responses, subsequently activating Th2-type adaptive immunity. This outcome enhances the release of type 2 cytokines, which in turn trigger skin inflammatory processes [35]. Notably, TSLP overexpression has been shown to drive type 2 inflammatory responses in mouse models, highlighting its pivotal role in the pathogenesis of skin inflammatory disorders [36]. This study highlights how TPA exposure provokes inflammation by stimulating crucial signaling cascades, resulting in elevated secretion of cytokines and chemokines. Such molecular events enhance immune cell recruitment and inflammatory activity, ultimately contributing to observable histopathological alterations [15]. The observed dose-dependent reduction in ear thickness, redness, and swelling can be attributed to the ability of CLE to modulate inflammatory mediators and suppress histopathological changes, including epidermal hyperplasia, hyperkeratosis, epidermal thickness, inflammatory cell infiltration, and tissue damage. Molecular analyses of ear tissues using RT-qPCR and western blotting revealed inflammatory patterns in ear swelling in edema mice, which were comparable to those examined in the PC group. Furthermore, CLE treatment markedly reduced COX-2 and iNOS levels in the ear tissues, highlighting its anti-inflammatory potential. Taken together, these findings suggest that CLE possesses considerable pharmacological potential as a natural anti-inflammatory agent for the skin.

Although our data demonstrate a clear local reduction of inflammation by topical CLE in the TPA-induced ear edema model, further studies using systemic inflammation models and systemic administration of CLE are required to determine whether CLE also exerts systemic anti-inflammatory effects. These experiments are beyond the scope of the present study and are planned for future work. Moreover, while the current results are encouraging, certain limitations should be acknowledged. For the further development of CLE as a therapeutic candidate, future research should address long-term safety, investigate systemic and chronic effects in diverse animal models, and conduct clinical testing to confirm efficacy and safety in humans.

5. Conclusions

Overall, the data suggest that CLE has significant bioactive potential as a natural anti-inflammatory agent for the skin. *In vivo*, CLE significantly alleviated inflammatory symptoms and modulated molecular mechanisms in TPA-induced ear edema, demonstrating its efficacy in a skin inflammation model. These outcomes collectively highlighted the pharmacological usefulness of CLE as a natural, plant-derived anti-inflammatory agent, offering a promising alternative for managing skin inflammation.

Availability of Data and Materials

The datasets used and analyzed during the current study are available from the corresponding author on reasonable request.

Author Contributions

AMKJ, and KGISK performed the research. KJ, JL, SL, and GA provided help and advice on the experiments. AMKJ, KGISK, KJ, JL, HMCBD, HMKR, LW, and JSK performed data analysis, curation, and visualization. SL, and GA provided funding and resources. SL, and GA were responsible for overall project supervision. AMKJ wrote the manuscript, and KGISK, SL, and GA contributed to its review and editing. All authors contributed to editorial changes in the manuscript. All authors read and approved the final manuscript. All authors have participated sufficiently in the work and agreed to be accountable for all aspects of the work.

Ethics Approval and Consent to Participate

All *in vivo* experiments were conducted following the guidelines of the Ethical Committee of Chonnam National University, South Korea (permission number CNU IACUC-YS-2022-7), and followed the recommendations of the American Veterinary Medical Association (AVMA).

Acknowledgment

Not applicable.

Funding

This work was supported by the Korea Institute of Planning and Evaluation for Technology in Food, Agriculture and Forestry (IPET) through the Technology Commercialization Support Program, funded by the Ministry of Agriculture, Food and Rural Affairs (MAFRA) (122052032HD030).

Conflict of Interest

The authors declare no conflict of interest. We confirmed that there is no conflict of interest between this study including its experimental conception and design, data collection, acquisition, analysis, and interpretation, and the institution “French Korea Aromatics Co., Ltd.”. Given his role as the Guest Editor, Lei Wang had no involvement in the peer review of this article and has no access to information regarding its peer review. Full responsibility for the editorial process for this article was delegated to Catarina Rosado.

Supplementary Material

Supplementary material associated with this article can be found, in the online version, at https://doi.org/10.31083/FBL42888.

References

[1] Fernando IPS, Dias MKHM, Madusanka DMD, Han EJ, Kim MJ, Jeon YJ, *et al*. Fucoidan refined by Sargassum confusum indicate protective effects suppressing photo-oxidative stress and skin barrier perturbation in UVB-induced human keratinocytes. International Journal of Biological Macromolecules. 2020; 164: 149–161. https://doi.org/10.1016/j.ijbiomac.2020.07.136.

[2] Jayawardena TU, Sanjeewa KKA, Wang L, Kim WS, Lee TK, Kim YT, *et al*. Alginic Acid from *Padina boryana* Abate Particulate Matter-Induced Inflammatory Responses in Keratinocytes and Dermal Fibroblasts. Molecules (Basel, Switzerland). 2020; 25: 5746. https://doi.org/10.3390/molecules25235746.

[3] Lee HJ, Hong YJ, Kim M. Angiogenesis in Chronic Inflammatory Skin Disorders. International Journal of Molecular Sciences. 2021; 22: 12035. https://doi.org/10.3390/ijms222112035.

[4] Tong LZ, Desai RM, Olsen R, Davis M. The Pathophysiology, Diagnosis and Management of Chronic Inflammatory Skin Diseases. Discovery Medicine. 2024; 36: 1933–1954. https://doi.org/10.24976/Discov.Med.202436189.180.

[5] Jayasinghe AMK, Han EJ, Kirindage KGIS, Fernando IPS, Kim EA, Kim J, *et al*. 3-Bromo-4,5-dihydroxybenzaldehyde Isolated from Polysiphonia morrowii Suppresses TNF-α/IFN-γ-Stimulated Inflammation and Deterioration of Skin Barrier in HaCaT Keratinocytes. Marine Drugs. 2022; 20: 563. https://doi.org/10.3390/md20090563.

[6] Rodríguez-Yoldi MJ. Anti-Inflammatory and Antioxidant Properties of Plant Extracts. Antioxidants (Basel, Switzerland). 2021; 10: 921. https://doi.org/10.3390/antiox10060921.

[7] Chaiyana W, Charoensup W, Sriyab S, Punyoyai C, Neimkhum W. Herbal Extracts as Potential Antioxidant, Anti-Aging, Anti-Inflammatory, and Whitening Cosmeceutical Ingredients. Chemistry & Biodiversity. 2021; 18: e2100245. https://doi.org/10.1002/cbdv.202100245.

[8] Jayasinghe AMK, Kirindage KGIS, Kim SH, Lee S, Jung K, Shim SY, *et al*. Protective effect of Curcuma longa L. leaves and pseudostems extract against 1-chloro-2,4-dinitrobenzene-induced atopic dermatitis in BALB/c mice. Journal of Ethnopharmacology. 2025; 338: 119138. https://doi.org/10.1016/j.jep.2024.119138.

[9] Rezvanirad A, Mardani M, Shirzad H, Ahmadzadeh SM, Asgary S, Naimi A, *et al*. Curcuma longa: A review of therapeutic effects in traditional and modern medical references. Journal of Chemical and Pharmaceutical Sciences. 2016; 9: 3438–3448.

[10] Verma RK, Kumari P, Maurya RK, Kumar V, Verma RB, Singh RK. Medicinal properties of turmeric (Curcuma longa L.): A review. International Journal of Chemical Studies. 2018; 6: 1354–1357.

[11] Kim S, Kim M, Kang MC, Lee HHL, Cho CH, Choi I, *et al*. Antioxidant Effects of Turmeric Leaf Extract against Hydrogen Peroxide-Induced Oxidative Stress In Vitro in Vero Cells and In Vivo in Zebrafish. Antioxidants (Basel, Switzerland). 2021; 10: 112. https://doi.org/10.3390/antiox10010112.

[12] Tran GH, Lee HD, Kim SH, Lee S, Lee S. Profiling of the leaves and stems of Curcuma longa using LC-ESI-MS and HPLC analysis. Journal of Applied Biological Chemistry. 2023; 66: 338–344.

[13] Jayasinghe AMK, Kirindage KGIS, Kim SH, Lee S, Kim KN, Kim EA, *et al*. Leaves and pseudostems extract of Curcuma longa attenuates immunoglobulin E/bovine serum albumin-stimulated bone marrow-derived cultured mast cell activation and passive cutaneous anaphylaxis in BALB/c mice. Journal of Ethnopharmacology. 2024; 321: 117529. https://doi.org/10.1016/j.jep.2023.117529.

[14] Kirindage KGIS, Jayasinghe AMK, Jang MS, Lee KJ, Yun HJ, Ahn G, *et al*. *Kjellmaniella crassifolia* Reduces Lipopolysaccharide-Induced Inflammation in Caco-2 Cells and Ameliorates Loperamide-Induced Constipation in Mice. Journal of Microbiology and Biotechnology. 2024; 34: 2565–2575. https://doi.org/10.4014/jmb.2407.07036.

[15] Kirindage KG, Jayasinghe AM, Han EJ, Han HJ, Kim KN, Wang L, *et al*. Phlorofucofuroeckol-A refined by edible brown algae Ecklonia cava indicates anti-inflammatory effects on TNF-α/IFN-γ-stimulated HaCaT keratinocytes and 12-O-tetradecanoylphorbol 13-acetate-induced ear edema in BALB/c mice. Journal of Functional Foods. 2023; 109: 105786.

[16] Maheshika Kumari Jayasinghe A, Yang HW, Gedara Isuru Sandanuwan Kirindage K, Jung K, Je JG, Wang L, *et al*. Fucosterol isolated from Sargassum horneri attenuates allergic responses in immunoglobulin E/bovine serum albumin-stimulated mast cells and passive cutaneous anaphylaxis in mice. International Immunopharmacology. 2024; 131: 111851. https://doi.org/10.1016/j.intimp.2024.111851.

[17] Stacey SK, McEleney M. Topical Corticosteroids: Choice and Application. American Family Physician. 2021; 103: 337–343.

[18] Michel P, Żbikowska HM, Rudnicka K, Gonciarz W, Krupa A, Gajewski A, *et al*. Anti-inflammatory, antioxidant and photoprotective activity of standardised Gaultheria procumbens L. leaf, stem, and fruit extracts in UVA-irradiated human dermal fibroblasts. Journal of Ethnopharmacology. 2024; 319: 117219. https://doi.org/10.1016/j.jep.2023.117219.

[19] Moradnia M, Mohammadkhani N, Azizi B, Mohammadi M, Ebrahimpour S, Tabatabaei-Malazy O, *et al*. The power of Punica granatum: A natural remedy for oxidative stress and inflammation; a narrative review. Journal of Ethnopharmacology. 2024; 330: 118243. https://doi.org/10.1016/j.jep.2024.118243.

[20] Calixto-Campos C, Carvalho TT, Hohmann MSN, Pinho-Ribeiro FA, Fattori V, Manchope MF, *et al*. Vanillic Acid Inhibits Inflammatory Pain by Inhibiting Neutrophil Recruitment, Oxidative Stress, Cytokine Production, and NFκB Activation in Mice. Journal of Natural Products. 2015; 78: 1799–1808. https://doi.org/10.1021/acs.jnatprod.5b00246.

[21] Zhu H, Liang QH, Xiong XG, Wang Y, Zhang ZH, Sun MJ, *et al*. Anti-Inflammatory Effects of p-Coumaric Acid, a Natural Compound of *Oldenlandia diffusa*, on Arthritis Model Rats. Evidence-based Complementary and Alternative Medicine: ECAM. 2018; 2018: 5198594. https://doi.org/10.1155/2018/5198594.

[22] Zhendong Y, Changjun C, Haocheng H, Qibin L, Dailing C, Linsong T, *et al*. Regulation of macrophage polarization and pyroptosis by 4-methylcatechol alleviates collagen-induced arthritis via Nrf2/HO-1 and NF-κB/NLRP3 signaling pathways. International Immunopharmacology. 2025; 146: 113855. https://doi.org/10.1016/j.intimp.2024.113855.

[23] Kim JH, Kim M, Kim JM, Lee MK, Seo SJ, Park KY. Afzelin suppresses proinflammatory responses in particulate matter-exposed human keratinocytes. International Journal of Molecular Medicine. 2019; 43: 2516–2522. https://doi.org/10.3892/ijmm.2019.4162.

[24] Kim MC, Kim SJ, Kim DS, Jeon YD, Park SJ, Lee HS, *et al*. Vanillic acid inhibits inflammatory mediators by suppressing NF-κB in lipopolysaccharide-stimulated mouse peritoneal macrophages. Immunopharmacology and Immunotoxicology. 2011; 33: 525–532. https://doi.org/10.3109/08923973.2010.547500.

[25] Pragasam SJ, Venkatesan V, Rasool M. Immunomodulatory

and anti-inflammatory effect of p-coumaric acid, a common dietary polyphenol on experimental inflammation in rats. Inflammation. 2013; 36: 169–176. https://doi.org/10.1007/s10753-012-9532-8.

[26] Zawawi NA, Ahmad H, Madatheri R, Fadilah NIM, Maarof M, Fauzi MB. Flavonoids as Natural Anti-Inflammatory Agents in the Atopic Dermatitis Treatment. Pharmaceutics. 2025; 17: 261. https://doi.org/10.3390/pharmaceutics17020261.

[27] Naruke A, Nakano R, Nunomura J, Suwabe Y, Nakano M, Namba S, *et al*. Tpl2 contributes to IL-1β-induced IL-8 expression via ERK1/2 activation in canine dermal fibroblasts. PloS One. 2021; 16: e0259489. https://doi.org/10.1371/journal.pone.0259489.

[28] Aliyu M, Zohora FT, Anka AU, Ali K, Maleknia S, Saffarioun M, *et al*. Interleukin-6 cytokine: An overview of the immune regulation, immune dysregulation, and therapeutic approach. International Immunopharmacology. 2022; 111: 109130. https://doi.org/10.1016/j.intimp.2022.109130.

[29] Jin SE, Seo CS, Jeon WY, Oh YJ, Shin HK, Jeong HG, *et al*. Evodiae Fructus extract suppresses inflammatory response in HaCaT cells and improves house dust mite-induced atopic dermatitis in NC/Nga mice. Scientific Reports. 2024; 14: 472. https://doi.org/10.1038/s41598-023-50257-3.

[30] Han JY, Lee YJ, Lim DW, Jung HJ, Kwon E, Hong J, *et al*. Cheungsam Seed Husk Extract Reduces Skin Inflammation through Regulation of Inflammatory Mediator in TNF-α/IFN-γ-Induced HaCaT Cells. Plants (Basel, Switzerland). 2024; 13: 1704. https://doi.org/10.3390/plants13121704.

[31] Razavi BM, Ghasemzadeh Rahbardar M, Hosseinzadeh H. A review of therapeutic potentials of turmeric (Curcuma longa) and its active constituent, curcumin, on inflammatory disorders, pain, and their related patents. Phytotherapy Research: PTR. 2021; 35: 6489–6513. https://doi.org/10.1002/ptr.7224.

[32] Kucuksezer UC, Ozdemir C, Yazici D, Pat Y, Mitamura Y, Li M, *et al*. The epithelial barrier theory: Development and exacerbation of allergic and other chronic inflammatory diseases. Asia Pacific Allergy. 2023; 13: 28–39. https://doi.org/10.5415/apallergy.0000000000000005.

[33] Peng G, Zhao W, Abudouwanli A, Sun Q, Yang M, Wang S, *et al*. Improvement of atopic dermatitis-like symptoms in a murine model via the chromogranin A-derived peptide catestatin. Allergology International: Official Journal of the Japanese Society of Allergology. 2025; 74: 563–571. https://doi.org/10.1016/j.alit.2025.01.001.

[34] Park SI, Lee J, Shin MS. Clinical study on itching relief caused by dry skin of cosmetics containing ceramide NP and guaiazulene in smart healthcare products. In Smart Healthcare Analytics: State of the Art (pp. 65–74). Springer Singapore: Singapore. 2021. https://doi.org/10.1007/978-981-16-5304-9_6.

[35] Beck LA, Cork MJ, Amagai M, De Benedetto A, Kabashima K, Hamilton JD, *et al*. Type 2 Inflammation Contributes to Skin Barrier Dysfunction in Atopic Dermatitis. JID Innovations: Skin Science from Molecules to Population Health. 2022; 2: 100131. https://doi.org/10.1016/j.xjidi.2022.100131.

[36] Akdis CA, Arkwright PD, Brüggen MC, Busse W, Gadina M, Guttman-Yassky E, *et al*. Type 2 immunity in the skin and lungs. Allergy. 2020; 75: 1582–1605. https://doi.org/10.1111/all.14318.